



A Journal of the Gesellschaft Deutscher Chemiker

Angewandte Chemie

GDCh

International Edition

www.angewandte.org

Accepted Article

Title: Fe-O Clusters Anchored on Nodes of Metal-Organic Frameworks for Direct Methane Oxidation

Authors: Wenshi Zhao, Yanan Shi, Yuheng Jiang, Xiaofei Zhang, Chang Long, Pengfei An, Yanfei Zhu, Shengxian Shao, Zhuang Yan, Guodong Li, and Zhiyong Tang

This manuscript has been accepted after peer review and appears as an Accepted Article online prior to editing, proofing, and formal publication of the final Version of Record (VoR). This work is currently citable by using the Digital Object Identifier (DOI) given below. The VoR will be published online in Early View as soon as possible and may be different to this Accepted Article as a result of editing. Readers should obtain the VoR from the journal website shown below when it is published to ensure accuracy of information. The authors are responsible for the content of this Accepted Article.

To be cited as: *Angew. Chem. Int. Ed.* 10.1002/anie.202013807

Link to VoR: <https://doi.org/10.1002/anie.202013807>

Fe-O Clusters Anchored on Nodes of Metal-Organic Frameworks for Direct Methane Oxidation

Wenshi Zhao, Yanan Shi, Yuheng Jiang, Xiaofei Zhang, Chang Long, Pengfei An, Yanfei Zhu, Shengxian Shao, Zhuang Yan, Guodong Li* and Zhiyong Tang*

- [a] W. Zhao, Y. Shi, Y. Jiang, Dr. X. Zhang, C. Long, Dr. Y. Zhu, S. Shao, Z. Yan, Prof. G. Li and Prof. Z. Tang
CAS Key Laboratory of Nanosystem and Hierarchical Fabrication, CAS Center for Excellence in Nanoscience, National Center for Nanoscience and Technology
Beijing 100190, P. R. China
E-mail: liguodong@nanoctr.cn, zytang@nanoctr.cn
- [b] W. Zhao, S. Shao, Z. Yan, Prof. G. Li and Prof. Z. Tang
School of Nanoscience and Technology, University of Chinese Academy of Sciences
Beijing 100049, P. R. China
- [c] Dr. P. An
Beijing Synchrotron Radiation Facility, Institute of High Energy Physics, Chinese Academy of Sciences
Beijing 100049, P. R. China

Supporting information for this article is given via a link at the end of the document.

Abstract: Direct methane oxidation into value-added organic oxygenates with high productivity under mild condition remains a great challenge. In this work, we show Fe-O clusters on nodes of metal-organic frameworks (MOFs) with tunable electronic state for direct methane oxidation into C1 organic oxygenates at 50°C. The Fe-O clusters are grafted onto inorganic Zr₆ nodes of UiO-66 (UiO stands for University of Oslo), while the organic terephthalic acid (H₂BDC) ligands of UiO-66 are partially substituted with monocarboxylic modulators of acetic acid (AA) or trifluoroacetic acid (TFA). Experiments and theoretical calculation disclose that the TFA group coordinated with Zr₆ node of UiO-66 enhances the oxidation state of adjacent Fe-O cluster due to its electron-withdrawing ability, promotes the activation of C-H bond of methane and increases its selective conversion, thus leading to the extraordinarily high C1 oxygenate yield of 4799 μmol g_{cat}⁻¹ h⁻¹ with 97.9% selectivity, ~8 times higher than those modulated with AA.

Direct conversion of methane into the value-added oxygenated chemicals, which is considered as the “holy grail” in catalysis, is economical and environmentally friendly but hardly implemented, because methane is characteristic of strong C-H bond (439 kJ/mol), negligible electron affinity, large ionization energy, and low polarizability.^[1] It always remains difficult to cleave the C-H bonds of methane and make it amenable for further chemical conversion. To date, many types of heterogeneous catalysts, such as the supported Fe or Cu catalysts, have come to the forefront of direct catalytic methane oxidation with various oxidants of N₂O, H₂O₂ and O₂.^[2] Unfortunately, the obtained target products are more active than methane and fully oxidized product of CO₂, usually giving rise to the low yield of organic oxygenates.^[3] Therefore, it is highly desirable to rationally design and synthesize the heterogeneous catalysts that can selectively activate the C-H bonds of methane while suppressing complete dehydrogenation and avoiding overoxidation.^[4]

Among various heterogeneous catalysts, MOFs, which are formed by self-assembly of metal ions or clusters with ditopic or polytopic organic linkers, are ideal candidates, due to their

intriguing features including large surface area, tunable pore dimensions, well-defined metal nodes, adjustable chemical composition and rich functionality.^[5] To be specific, the metal nodes of MOFs are often coordinated with -OH and -OH₂ groups that could further act as the anchoring sites for active components, offering many opportunities for precise design of the catalyst at the molecular level.^[6] In this work, we demonstrate that Fe-O clusters on Zr₆ nodes of UiO-66 modulated with TFA are able to effectively activate the inert C-H bond of methane and simultaneously catalyze methane oxidation with H₂O₂ as the oxidant. The C1 organic oxygenates are acquired with high yield and good selectivity under mild condition.

In brief, grafting of Fe-O clusters onto Zr₆ nodes of UiO-66 involves three steps: (1) competitive coordination of Zr⁴⁺ ion with monocarboxylic modulator over bicarboxylic H₂BDC ligand to form the variant UiO-66,^[7] (2) abstracting hydrogen atoms from -OH/-OH₂ groups in UiO-66,^[8] (3) anchoring Fe-O clusters to obtain the catalysts (Figure 1a). In detail, dissolution of ZrCl₄ and H₂BDC in *N,N*-dimethylformamide (DMF) solution was carried out, followed by addition of TFA and solvothermal treatment to achieve the UiO-66 with composition of Zr₆O_{4.17}(OH)_{3.83}(BDC)_{4.29}(HCOO)_{0.75}(TFA)_{2.50} (Figure S1), named as UiO-66(2.5TFA). After that, the hydrogen atoms of -OH and -OH₂ groups in UiO-66(2.5TFA) were removed.^[8] Finally, the obtained solid was transferred into FeCl₂ tetrahydrofuran (THF) solution to get the brown solid products, denoted as UiO-66(2.5TFA)-Fe. Furthermore, nuclear magnetic resonance (NMR) spectra show that after grafting Fe sites, the TFA groups are still well coordinated with Zr₆ nodes (Figure S2). As the contrast sample, another UiO-66 was synthesized by reacting Zr⁴⁺ ion and H₂BDC with AA, and its composition was determined as Zr₆O_{4.33}(OH)_{3.67}(BDC)_{5.34}(HCOO)_{0.62}(AA)_{0.37}, called as UiO-66(0.37AA) (Figure S3). Similarly, it was subjected to abstracting hydrogen and anchoring Fe-O clusters to obtain the UiO-66(0.37AA)-Fe sample.

COMMUNICATION

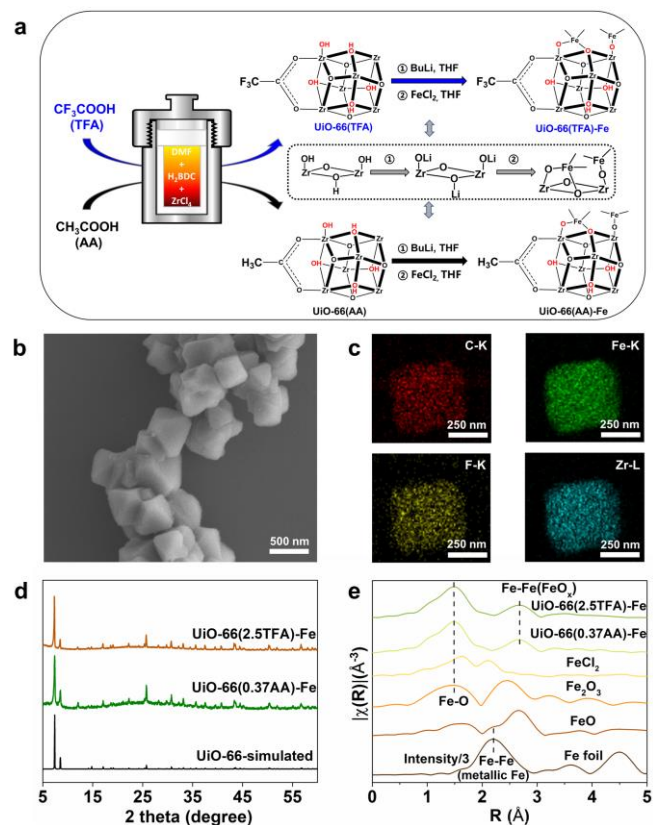


Figure 1. (a) Scheme of synthesizing Zr_6 nodes coordinated with TFA or AA and then anchoring Fe sites on Zr_6 nodes. (b) SEM image of UiO-66(2.5TFA)-Fe. (c) Transmission electron microscopy energy-dispersive X-ray spectroscopy (TEM-EDX) mapping images of UiO-66(2.5TFA)-Fe. (d) Powder XRD patterns of UiO-66(2.5TFA)-Fe, UiO-66(0.37AA)-Fe and simulated UiO-66. (e) Fourier transformed Fe *K*-edge EXAFS spectra in R-space collected on UiO-66(2.5TFA)-Fe, UiO-66(0.37AA)-Fe, $FeCl_2$, Fe_2O_3 , FeO and Fe foil under ambient condition (not corrected for phase shift).

The morphology and structure of as-prepared UiO-66(2.5TFA)-Fe and UiO-66(0.37AA)-Fe samples are investigated. Scanning electron microscopy (SEM) observation shows that both nanoparticles have rather uniform sizes of 340 ± 46 nm for UiO-66(2.5TFA)-Fe and 165 ± 17 nm for UiO-66(0.37AA)-Fe (Figures 1b, S4 and S5). The element mapping images indicate that the Fe element is uniformly distributed inside UiO-66(2.5TFA)-Fe and UiO-66(0.37AA)-Fe samples (Figures 1c, S4 and S5), and the quantitative measurement reveals 2.2 wt% and 3.0 wt% Fe inside, respectively. Powder X-ray diffraction (XRD) patterns display that crystal structure of UiO-66(2.5TFA)-Fe and UiO-66(0.37AA)-Fe is in good agreement with that of typical UiO-66, validating well maintenance of the cubic close packed structure of UiO-66; in addition, no obvious XRD peaks of Fe sites are discerned likely due to their extremely small size and low loading (Figure 1d). As shown in Fourier transform infrared (FTIR) spectra (Figure S6), after anchoring Fe-O clusters, the intensity of O-H peaks become weaker for both UiO-66(2.5TFA)-Fe and UiO-66(0.37AA)-Fe,^[6b] suggesting successful formation of Fe-O clusters on the Zr_6 nodes. The local structure of the attached Fe-O clusters is elucidated by X-ray photoelectron spectroscopy (XPS) and X-ray absorption spectroscopy (XAS). XPS spectra imply that the Cl from $FeCl_2$ precursor is not incorporated in UiO-66(2.5TFA)-Fe (Figure S7). Fourier transformed Fe *K*-edge extended X-ray absorption fine

structure (EXAFS) spectra in R-space demonstrate that Fe sites in UiO-66(2.5TFA)-Fe and UiO-66(0.37AA)-Fe possess the similar local structure (Figure 1e), which is close to that of FeO and Fe_2O_3 standards based on comparison of the peaks at 1.46 Å (the first oxygen neighbor around Fe) and at 2.66 Å (Fe-Fe from the second neighbor correlation). The quantitative fitting further discloses that the Fe-Fe coordination number is low with an average Fe-Fe distance of 3.07 Å and an average Fe-O separation of 1.96 Å (Table S1). N_2 adsorption-desorption isotherms manifest that the specific surface areas are $945 \text{ m}^2 \text{ g}^{-1}$ for UiO-66(2.5TFA)-Fe and $1193 \text{ m}^2 \text{ g}^{-1}$ for UiO-66(2.5TFA), as well as $686 \text{ m}^2 \text{ g}^{-1}$ for UiO-66(0.37AA)-Fe and $971 \text{ m}^2 \text{ g}^{-1}$ for UiO-66(0.37AA) (Figure S8 and Table S2).

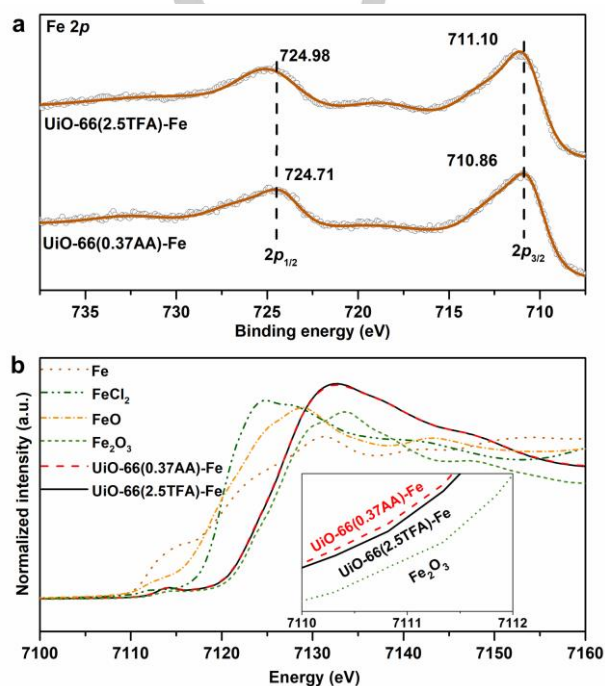


Figure 2. Characterization of oxidation state of Fe sites in different samples. (a) Fe 2*p* level profiles of UiO-66(2.5TFA)-Fe and UiO-66(0.37AA)-Fe samples. (b) Fe *K*-edge XANES spectra of UiO-66(2.5TFA)-Fe, UiO-66(0.37AA)-Fe, Fe_2O_3 , FeO, $FeCl_2$ and Fe foil.

XPS measurement was performed on UiO-66(2.5TFA)-Fe along with UiO-66(0.37AA)-Fe (Figures 2a and S9). The Fe $2p_{3/2}$ binding energy is located at 711.10 eV for UiO-66(2.5TFA)-Fe, higher than 710.86 eV for UiO-66(0.37AA)-Fe (Figure 2a). This difference is further confirmed by X-ray absorption near-edge structure (XANES) spectroscopy. The Fe *K*-edge XANES of UiO-66(2.5TFA)-Fe shifts toward higher energy compared with UiO-66(0.37AA)-Fe (inset in Figure 2b), highlighting the higher oxidation state of Fe sites in UiO-66(2.5TFA)-Fe. This is attributed to the electronegativity of F element (4.1) higher than H element (2.1),^[9] thus leading to the stronger electron-withdrawing effect of TFA on Fe-O clusters than AA. Besides, the position of the pre-edge peaks of both UiO-66(2.5TFA)-Fe and UiO-66(0.37AA)-Fe is located in the middle between FeO and Fe_2O_3 reference compounds (Figure 2b), suggesting that the valent state of the Fe sites is between +2 and +3 with a distorted octahedral symmetry.^[10]

COMMUNICATION

Table 1. Direct methane oxidation catalyzed by different catalysts.^[a]

Entry	Catalysts	Metal ^[b] (wt%)	C1 organic products ($\mu\text{mol g}_{\text{cat}}^{-1} \text{h}^{-1}$) ^[c]					CO ₂ ($\mu\text{mol g}_{\text{cat}}^{-1} \text{h}^{-1}$) ^[c]
			CH ₃ OH	CH ₃ OOH	HOCH ₂ OOH	HCOOH	Total amount	
1	UiO-66(2.5TFA)-Fe	2.2	258.7	401.0	1029.8	3109.7	4799.2	105
2	UiO-66(1TFA)-Fe	2.2	221.6	260.0	423.2	1043.2	1948.0	72
3	UiO-66(1.24AA)-Fe	3.3	79.6	154.4	148.0	226.8	608.8	33
4	UiO-66(0.37AA)-Fe	3.0	37.0	44.8	33.6	483.8	599.2	104
5	UiO-66-Fe	2.1	52.6	60.5	35.3	367.9	516.3	22
6	Without catalyst ^[d]	-	0	0	0	0	0	0.5
7	UiO-66(0.37AA)-Fe ^[e]	3.0	50.4	86.2	63.8	398.2	598.6	240
8	Fe ₂ O ₃	36.8	51.6	59.2	162.8	0	273.6	92
9	FeO	46.7	0	0	0	0	0	16
10	UiO-66(2.5TFA)-Cu	1.3	5.6	21.2	0	0	26.8	72
11	UiO-66(2.5TFA)-Co	2.4	14.4	57.2	11.8	0	83.4	0

[a] Reaction condition: catalyst (25 mg), 3 MPa CH₄, 0.3 mL 30wt% H₂O₂ in 9.7 mL D₂O, 50°C, 1 h. [b] Metal contents including Fe, Cu or Co were detected by ICP-MS. [c] The yield of the obtained products was calculated based on the weight of whole catalyst. [d] The yield of CO₂ is 0.5 $\mu\text{mol h}^{-1}$. [e] 5.26 mg sodium trifluoroacetate was added to the reaction solution.

The catalytic performance of UiO-66(2.5TFA)-Fe was evaluated on direct methane oxidation in water using H₂O₂ as the oxidant at 3 MPa CH₄ and 50°C for 1 h. A series of contrast samples including UiO-66(1TFA)-Fe, UiO-66(1.24AA)-Fe, UiO-66(0.37AA)-Fe, UiO-66-Fe, UiO-66(2.5TFA), UiO-66(1TFA), UiO-66(1.24AA) and UiO-66(0.37AA) were also synthesized and tested (Figures S10-S16). Without Fe-O clusters anchored on Zr₆ nodes, almost no activity is found (Table 1, entry 6, and Figure S17). On the contrary, Fe-O clusters on Zr₆ nodes of UiO-66 with or without modulators could catalyze methane oxidation into C1 products including CH₃OH, CH₃OOH, HOCH₂OOH and HCOOH, which are confirmed by ¹³C-NMR spectrum of the obtained products from ¹³CH₄ substrate as well as ¹H-NMR spectrum without adding substrate (Figure S18). When UiO-66-Fe is used as catalyst, the C1 organic products are 52.6 $\mu\text{mol g}_{\text{cat}}^{-1} \text{h}^{-1}$ CH₃OH, 60.5 $\mu\text{mol g}_{\text{cat}}^{-1} \text{h}^{-1}$ CH₃OOH, 35.3 $\mu\text{mol g}_{\text{cat}}^{-1} \text{h}^{-1}$ HOCH₂OOH and 367.9 $\mu\text{mol g}_{\text{cat}}^{-1} \text{h}^{-1}$ HCOOH, and the total amount of C1 organic oxygenates is 516.3 $\mu\text{mol g}_{\text{cat}}^{-1} \text{h}^{-1}$ (Table 1, entry 5, Figure S19). Gas product CO₂ is observed with a value of 22 $\mu\text{mol g}_{\text{cat}}^{-1} \text{h}^{-1}$. When UiO-66(0.37AA)-Fe is used as catalyst, the organic products are achieved with 37.0 $\mu\text{mol g}_{\text{cat}}^{-1} \text{h}^{-1}$ CH₃OH, 44.8 $\mu\text{mol g}_{\text{cat}}^{-1} \text{h}^{-1}$ CH₃OOH, 33.6 $\mu\text{mol g}_{\text{cat}}^{-1} \text{h}^{-1}$ HOCH₂OOH and 483.8 $\mu\text{mol g}_{\text{cat}}^{-1} \text{h}^{-1}$ HCOOH (Figure S20a), so the total amount of C1 organic oxygenates is 599.2 $\mu\text{mol g}_{\text{cat}}^{-1} \text{h}^{-1}$ (Table 1, entry 4). Meanwhile, the yield of CO₂ is 104 $\mu\text{mol g}_{\text{cat}}^{-1} \text{h}^{-1}$, and thus the selectivity of C1 organic oxygenates is around 85.2%. Notably, when TFA is coordinated with Zr₆ node of UiO-66-Fe, the catalytic performance is significantly enhanced. UiO-66(1TFA)-Fe exhibits the productivity of 1948 $\mu\text{mol g}_{\text{cat}}^{-1} \text{h}^{-1}$ for C1 organic oxygenates with the selectivity of 96.4% (Table 1, entry 2 and Figure S20b). More impressively, UiO-66(2.5TFA)-Fe shows the much higher yield of 4799.2 $\mu\text{mol g}_{\text{cat}}^{-1} \text{h}^{-1}$ for C1 organic oxygenates with a remarkable selectivity of 97.9%, and the productivity of CO₂ is only 105 $\mu\text{mol g}_{\text{cat}}^{-1} \text{h}^{-1}$ (Table 1, entry 1, Figures S21 and S22). In detail, the C1 organic oxygenate products include 258.7 $\mu\text{mol/g}_{\text{cat}} \text{h}$ CH₃OH, 401.0 $\mu\text{mol g}_{\text{cat}}^{-1} \text{h}^{-1}$ CH₃OOH, 1029.8 $\mu\text{mol g}_{\text{cat}}^{-1} \text{h}^{-1}$ HOCH₂OOH and 3109.7 $\mu\text{mol g}_{\text{cat}}^{-1} \text{h}^{-1}$ HCOOH. Evidently, the yield of C1 organic oxygenates over UiO-66(2.5TFA)-Fe is nearly 8 times

higher than that over UiO-66(0.37AA)-Fe. It deserves to be pointed out that after the catalytic reaction, both shape and crystal structure of UiO-66(2.5TFA)-Fe are well kept and no aggregation of Fe-O clusters is found (Figure S23). Notably, in comparison with the state-of-the-art reported heterogeneous catalysts, UiO-66(2.5TFA)-Fe displays the superior activity and high selectivity towards C1 organic oxygenates (Table S3).

In addition, FeO and Fe₂O₃ are used as the contrast catalysts for methane oxidation. No C1 organic oxygenates is discerned for FeO (Table 1, entry 9, Figure S24a), while Fe₂O₃ exhibits very low activity and the yield of C1 organic oxygenates is only 273.6 $\mu\text{mol g}_{\text{cat}}^{-1} \text{h}^{-1}$ (Table 1, entry 8, Figure S24b). The major disadvantage of Fe₂O₃ is its small specific surface area of 36.8 m² g⁻¹ (Figure S25), which offers much less active sites for catalytic reactions compared with porous MOFs. Another reason is that the TFA group coordinated with Zr₆ nodes of UiO-66 contributes to the significantly enhanced catalytic activity of the adjacent Fe-O clusters for generating C1 organic oxygenate products. To evidence above, TFA anions were added into the reaction solution when UiO-66(0.37AA)-Fe was used as catalyst. The yield of C1 organic oxygenate products is 598.6 $\mu\text{mol g}_{\text{cat}}^{-1} \text{h}^{-1}$, and no considerable improvement is discerned with respect to UiO-66(0.37AA)-Fe (Table 1, entry 7 vs. 4, Figure S26). This result suggests that the direct incorporation of TFA modulator in UiO-66 is necessary to increase the catalytic performance of Fe-O clusters.

Alternatively, more AA modulators are coordinated with Zr₆ nodes of UiO-66 to obtain the contrast sample, UiO-66(1.24AA)-Fe, for catalytic methane oxidation (Figures S12 and S13). XPS spectra also indicate that Fe 2p_{3/2} binding energy in UiO-66(1.24AA)-Fe is almost the same with UiO-66(0.37AA)-Fe (Figure S27). When UiO-66(1.24AA)-Fe is used as the catalysts, the yield of C1 organic oxygenate products is 608.8 $\mu\text{mol g}_{\text{cat}}^{-1} \text{h}^{-1}$, very close to 599.2 $\mu\text{mol g}_{\text{cat}}^{-1} \text{h}^{-1}$ obtained with UiO-66(0.37AA)-Fe (Table 1, entry 3 vs. 4, Figure S28).

Except for Fe sites, other metal sites anchored on Zr₆ nodes of UiO-66(2.5TFA) are fabricated, such as UiO-66(2.5TFA)-Cu and UiO-66(2.5TFA)-Co (Figures S29 and S30). UiO-66(2.5TFA)-Cu

COMMUNICATION

gives rise to the yield of $26.8 \mu\text{mol g}_{\text{cat}}^{-1} \text{h}^{-1}$ for C1 organic oxygenates (Table 1, entry 10), while the productivity of $83.4 \mu\text{mol g}_{\text{cat}}^{-1} \text{h}^{-1}$ for C1 organic oxygenates is obtained with UiO-66(2.5TFA)-Co (Table 1, entry 11).

It needs to be stressed that small amount of formic species is likely formed on Zr_6 nodes in the original catalyst, due to decomposition of DMF into formic acid during synthesis of UiO-66 samples (Figure S1).^[7] To exclude its influence on final products, contrast experiment was performed. No C1 organic products is detected over UiO-66(2.5TFA)-Fe without adding methane, indicating that coordinated HCOO^- group would not leak from the Zr_6 nodes (Figure S18b).

To investigate the mechanism of direct methane oxidation into C1 oxygenated products, electron paramagnetic resonance (EPR) experiments with 5,5'-dimethyl-1-pyrroline-N-oxide (DMPO) as a radical trapping agent were performed. Without adding methane, strong $\bullet\text{OH}$ signals are distinguished, indicating that H_2O_2 is activated by UiO-66(2.5TFA)-Fe (Figure 3a). After adding methane into the reaction solution, the strong $\bullet\text{OH}$ signals remain but in absence of $\bullet\text{CH}_3$ peaks, implying that as-generated $\bullet\text{CH}_3$ reacts with the rich $\bullet\text{OH}$ quickly.^[2c] When methanol is added into the reaction solution instead of methane, $\bullet\text{OH}$ and $\bullet\text{CH}_2\text{OH}$ are detected in the solution (Figure 3b); meanwhile, HOCH_2OOH and HCOOH are also produced, similar as those obtained from direct catalytic methane oxidation (Figure 3c). This result suggests that CH_3OH and CH_3OOH are produced from methane firstly and then further oxidized into HOCH_2OOH and HCOOH . Altogether, EPR and NMR characterizations reveal a radical reaction process for direct methane oxidation into C1 oxygenates with H_2O_2 as the oxidant.^[11]

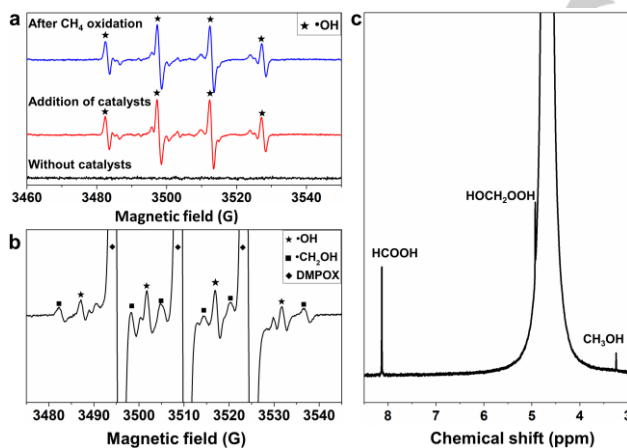


Figure 3. (a) EPR spectra of methane oxidation reaction catalyzed by UiO-66(2.5TFA)-Fe with H_2O_2 as oxidant. (b) EPR spectra of the CH_3OH oxidation reaction catalyzed by UiO-66(2.5TFA)-Fe with H_2O_2 as oxidant and (c) NMR spectra of the resultant solution.

Based on above and the reported works,^[2c, 12] it is generally accepted that H_2O_2 is firstly decomposed into active oxygen species and H_2O catalyzed by Fe-O clusters (Figure S31). Subsequently, methane is activated into $\bullet\text{CH}_3$ by active oxygen species on Fe-O clusters, and then $\bullet\text{CH}_3$ reacts with $\bullet\text{OH}$ and $\bullet\text{OOH}$ to produce CH_3OH and CH_3OOH , respectively. The C-H bond of as-formed CH_3OH might be further activated to generate $\bullet\text{CH}_2\text{OH}$ that combines $\bullet\text{OOH}$ to form HOCH_2OOH . Finally HOCH_2OOH is converted to HCOOH catalyzed by Fe-O clusters

(Figures 4a and S32). Theoretical calculation demonstrates that UiO-66(TFA)-Fe possesses the reduced energy of -3.259 eV for H_2O_2 activation compared with -2.586 eV over UiO-66-Fe, mainly due to the higher oxidation state of Fe sites in the UiO-66(TFA)-Fe (Figure 4b). As manifested in Figure 4c, the activation of first C-H bond of methane is the rate-determining step, consistent with the reported work.^[4] Noteworthy, in regard of the transit state $[\text{Fe}\cdots\text{H}\cdots\text{CH}_3]$ in the first C-H bond activation, the energy barrier of 0.372 eV over UiO-66(TFA)-Fe is lower than 0.603 eV over UiO-66-Fe, highlighting that UiO-66(TFA)-Fe is more active than UiO-66-Fe. Moreover, the reaction energy for each step over UiO-66(TFA)-Fe is lower than that over UiO-66-Fe, again indicating that UiO-66(TFA)-Fe is more active for methane oxidation towards C1 organic oxygenates (Figure 4c). To further differentiate the capability of both samples on first C-H bond activation, control experiments at a low temperature of 4°C are performed. No activity is found over UiO-66-Fe, but C1 organic products are obtained over UiO-66(2.5TFA)-Fe (Figure S33), indicating that it is easier to activate the first C-H bond by UiO-66(2.5TFA)-Fe than UiO-66-Fe.

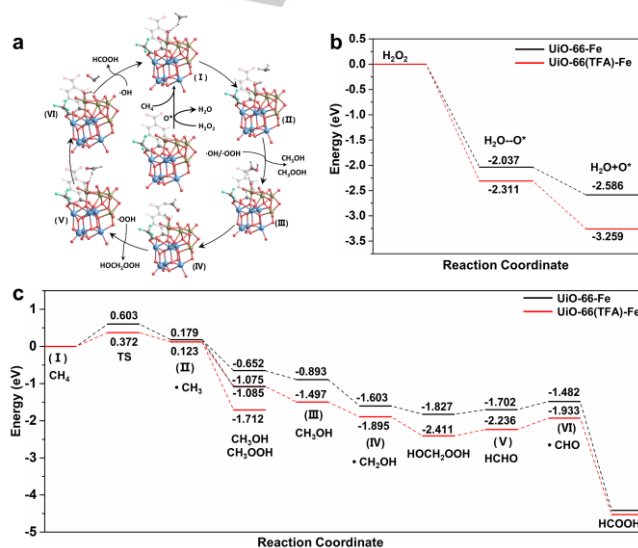


Figure 4. Reaction pathway of direct methane oxidation and theoretical calculation. (a) Scheme of reaction pathway for direct methane oxidation catalyzed by UiO-66(TFA)-Fe. (b) Relative energy for H_2O_2 activation over UiO-66(TFA)-Fe and UiO-66-Fe. (c) Relative energy for each step of direct methane oxidation into C1 products over UiO-66(TFA)-Fe and UiO-66-Fe. Color scheme: light gray for hydrogen, dark gray for carbon, green for fluorine, red for oxygen, blue for zirconium and brown for iron.

In summary, the efficient and selective oxidation of methane is successfully realized by Fe-O clusters on Zr_6 nodes of UiO-66 modulated with TFA. The increased oxidation state of Fe-O clusters coupled with TFA groups synergistically endows their higher activity towards activating both methane and H_2O_2 , thus resulting in high yield of C1 organic oxygenates. This work will open the avenues for molecular design of diverse coordination architectures in heterogeneous catalysts for important but challengeable reactions.

Acknowledgements

COMMUNICATION

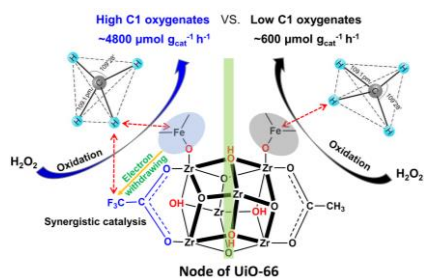
The authors acknowledge financial support from the Strategic Priority Research Program of Chinese Academy of Sciences (XDB36000000, Z.Y.T. and G.D.L.), National Key Basic Research Program of China (2016YFA0200700, Z.Y.T.), National Natural Science Foundation of China (92056204, 21890381 and 21721002, Z.Y.T.; 21722102 and 51672053, G.D.L.), Beijing Natural Science Foundation (2182087, G.D.L.), Frontier Science Key Project of Chinese Academy of Sciences (QYZDJ-SSW-SLH038, Z.Y.T.), and K. C. Wong Education Foundation (Z.Y.T.), and Youth Innovation Promotion Association CAS (2016036, G.D.L.).

Keywords: iron • methane • metal-organic frameworks • trifluoroacetic acid • C1 oxygenate

- [1] a) N. J. Gunsalus, A. Koppaka, S. H. Park, S. M. Bischof, B. G. Hashiguchi, R. A. Periana, *Chem. Rev.* **2017**, *117*, 8521–8573; b) B. A. Arndtsen, R. G. Bergman, T. A. Mobley, T. H. Peterson, *Acc. Chem. Res.* **1995**, *28*, 154–162; c) P. Schwach, X. Pan, X. Bao, *Chem. Rev.* **2017**, *117*, 8497–8520.
- [2] a) P. Tomkins, M. Ranocchiari, J. A. van Bokhoven, *Acc. Chem. Res.* **2017**, *50*, 418–425; b) C. Hammond, M. M. Forde, M. H. Ab Rahim, A. Thetford, Q. He, R. L. Jenkins, N. Dimitratos, J. A. Lopez-Sanchez, N. F. Dummer, D. M. Murphy, A. F. Carley, S. H. Taylor, D. J. Willock, E. E. Stangland, J. Kang, H. Hagen, C. J. Kiely, G. J. Hutchings, *Angew. Chem.* **2012**, *124*, 5219–5223; *Angew. Chem. Int. Ed.* **2012**, *51*, 5129–5133; c) X. Cui, H. Li, Y. Wang, Y. Hu, L. Hua, H. Li, X. Han, Q. Liu, F. Yang, L. He, X. Chen, Q. Li, J. Xiao, D. Deng, X. Bao, *Chem* **2018**, *4*, 1902–1910; d) J. Baek, B. Rungtaweevoranit, X. Pei, M. Park, S. C. Fakra, Y.-S. Liu, R. Matheu, S. A. Alshmirri, S. Alshehri, C. A. Trickett, G. A. Somorjai, O. M. Yaghi, *J. Am. Chem. Soc.* **2018**, *140*, 18208–18216.
- [3] a) R. G. Bergman, *Nature* **2007**, *446*, 391–393; b) A. I. Olivios-Suarez, Á. Szécsényi, E. J. M. Hensen, J. Ruiz-Martinez, E. A. Pidko, J. Gascon, *ACS Catal.* **2016**, *6*, 2965–2981.
- [4] B. L. Conley, W. J. Tenn, K. J. H. Young, S. K. Ganesh, S. K. Meier, V. R. Ziatdinov, O. Mironov, J. Oxgaard, J. Gonzales, W. A. Goddard, R. A. Periana, *J. Mol. Catal. A Chem* **2006**, *251*, 8–23.
- [5] a) J. Lee, O. K. Farha, J. Roberts, K. A. Scheidt, S. T. Nguyen, J. T. Hupp, *Chem. Soc. Rev.* **2009**, *38*, 1450–1459; b) H. Furukawa, K. E. Cordova, M. O’Keeffe, O. M. Yaghi, *Science* **2013**, *341*, 1230444; c) W. Zhang, W. Shi, W. Ji, H. Wu, Z. Gu, P. Wang, X. Li, P. Qin, J. Zhang, Y. Fan, T. Wu, Y. Fu, W. Zhang, F. Huo, *ACS Catal.* **2020**, *10*, 5805–5813; d) Z. Niu, X. Cui, T. Pham, P. C. Lan, H. Xing, K. A. Forrest, L. Wojtas, B. Space, S. Ma, *Angew. Chem.* **2019**, *131*, 10244–10247; *Angew. Chem. Int. Ed.* **2019**, *58*, 10138–10141; e) Y. Zheng, S.-Z. Qiao, *Natl. Sci. Rev.* **2018**, *5*, 626–627.
- [6] a) J. Liu, J. Ye, Z. Li, K.-i. Otake, Y. Liao, A. W. Peters, H. Noh, D. G. Truhlar, L. Gagliardi, C. J. Cramer, O. K. Farha, J. T. Hupp, *J. Am. Chem. Soc.* **2018**, *140*, 11174–11178; b) J. Liu, Z. Li, X. Zhang, K.-i. Otake, L. Zhang, A. W. Peters, M. J. Young, N. M. Bedford, S. P. Letourneau, D. J. Mandia, J. W. Elam, O. K. Farha, J. T. Hupp, *ACS Catal.* **2019**, *9*, 3198–3207; c) D. Chen, W. Yang, L. Jiao, L. Li, S.-H. Yu, H.-L. Jiang, *Adv. Mater.* **2020**, *32*, 2000041; d) X. Li, B. Zhang, L. Tang, T. W. Goh, S. Qi, A. Volkov, Y. Pei, Z. Qi, C.-K. Tsung, L. Stanley, W. Huang, *Angew. Chem.* **2017**, *129*, 16589–16593; *Angew. Chem. Int. Ed.* **2017**, *56*, 16371–16375; e) X. Li, T. W. Goh, L. Li, C. Xiao, Z. Guo, X. C. Zeng, W. Huang, *ACS Catal.* **2016**, *6*, 3461–3468; f) Z. Li, T. M. Rayder, L. Luo, J. A. Byers, C.-K. Tsung, *J. Am. Chem. Soc.* **2018**, *140*, 8082–8085; g) Z. Niu, W. D. C. Bhagya Gunatilleke, Q. Sun, P. C. Lan, J. Perman, J.-G. Ma, Y. Cheng, B. Aguila, S. Ma, *Chem* **2018**, *4*, 2587–2599; h) C. Xu, Y. Pan, G. Wan, H. Liu, L. Wang, H. Zhou, S.-H. Yu, H.-L. Jiang, *J. Am. Chem. Soc.* **2019**, *141*, 19110–19117.
- [7] G. C. Shearer, S. Chavan, S. Bordiga, S. Svelle, U. Olsbye, K. P. Lillerud, *Chem. Mater.* **2016**, *28*, 3749–3761.
- [8] K. Manna, P. Ji, Z. Lin, F. X. Greene, A. Urban, N. C. Thacker, W. Lin, *Nat. Commun.* **2016**, *7*, 12610.
- [9] E. J. Little, Jr., M. M. Jones, *J. Chem. Education* **1960**, *37*, 231–233.
- [10] J. Xie, R. Jin, A. Li, Y. Bi, Q. Ruan, Y. Deng, Y. Zhang, S. Yao, G. Sankar, D. Ma, J. Tang, *Nat. Catal.* **2018**, *1*, 889–896.
- [11] M. H. Ab Rahim, M. M. Forde, R. L. Jenkins, C. Hammond, Q. He, N. Dimitratos, J. A. Lopez-Sanchez, A. F. Carley, S. H. Taylor, D. J. Willock, D. M. Murphy, C. J. Kiely, G. J. Hutchings, *Angew. Chem.* **2013**, *125*, 1318–1322; *Angew. Chem. Int. Ed.* **2013**, *52*, 1280–1284.
- [12] a) A. A. Latimer, A. R. Kulkarni, H. Aljama, J. H. Montoya, J. S. Yoo, C. Tsai, F. Abild-Pedersen, F. Studd, J. K. Nørskov, *Nat. Mater.* **2017**, *16*, 225–229; b) Á. Szécsényi, G. Li, J. Gascon, E. A. Pidko, *ACS Catal.* **2018**, *8*, 7961–7972; c) Q. Shen, C. Cao, R. Huang, L. Zhu, X. Zhou, Q. Zhang, L. Gu, W. Song, *Angew. Chem.* **2020**, *132*, 1232–1235; *Angew. Chem. Int. Ed.* **2020**, *59*, 1216–1219.

COMMUNICATION

Entry for the Table of Contents



We successfully synthesize Fe-O clusters on nodes of UiO-66 simultaneously coordinated with trifluoroacetic acid (TFA) or acetic acid (AA) for direct methane oxidation. The TFA group coordinated with Zr₆ node of UiO-66 enhances the oxidation state of adjacent Fe-O cluster, promotes the activation of C-H bond of methane and increases its selective conversion into the extraordinarily high C1 oxygenates with respect to those coordinated with AA.